RENORMALIZATION GROUP METHOD: INFLUENCE OF PACKING DENSITY OF AXONS ON DIFFUSIVITY IN ENHANCED BASSER-SEN MODEL OF THE BRAIN WHITE MATTER

O. P. Posnansky[1], and N. J. Shah[1,2]

[1]Institute of Neuroscience and Medicine - 4, Medical Imaging Physics, Forschungszentrum Juelich, GmbH, 52425 Juelich, Germany, [2]Deparment of Neurology, Faculty of Medicine, RWTH Aachen University, 52074 Aachen, Germany

1. Introduction: The signal in diffusion-weighted (*DW*) MRI experiments is exquisitely sensitive to water molecular dynamics in the local geometrical and physiological environment. Determining whether it is possible to infer the specific mechanisms that underlie changes in the DW-MRI signal is an intense area of investigation and could lead to new modelling approaches for generating *DW*-MRI contrasts that are specific to particular white matter degeneration processes. However, the complexity of the diffusion behaviour due to compartmentalization, exchange, restrictions and anisotropy imposed by cellular microstructure, hinders the establishment of relations between dynamics and structure in a quantitative manner. In recent years, increasing efforts have been made to interpret diffusion in brain tissue using geometrical models [1,2]. In our work, the renormalization group (*RG*) method of an *enhanced Basser-Sen* (*BS*) model [3] was performed taking into account possible different packing densities of axons. Various tessellations were modelled using symmetry properties of the Wigner-Seitz (*WS*) cell with a random probability of occupation.

2. Methods: Diffusion in brain white matter was modelled in a cross-sectional raster filled with infinitely long, parallel-aligned cylinders representing myelinated axons immersed in an extracellular matrix. Following the *BS* model, we characterize axons by D_m (myelin-sheath diffusion), D_a (axon diffusion) and corresponding proton densities c_a, c_m, which have outer (R_m) and inner (R_a) radii. Such a compartment is immersed in an extra-cellular space with diffusion D_e, proton density c_e and linear size L. The properties of all components are colour coded as in Fig.1. If we suppose that white matter structure can be tessellated by *WS* cells with different symmetries, for example, square (Fig.2a) and hexagonal (Fig.2b) then it is possible to calculate the diffusive properties using the *BS* model. The two types of *WS* cells can be randomly distributed on the lattice with a probability p that a *WS* cell is empty and $(1-p)$ that a *WS* contains fibres. In Fig.3a,b, a black *WS* cell indicates fibre occupation and the overlaid yellow lattice is a dual to the original one. Vertices of the dual lattice are assigned to the random *WS* cells. Random occupation of the *WS* cells is the opposite of the ordered spatial distribution of fibres described in the BS model. On the square and hexagonal lattices with randomly occupied cells it is possible to outline a *RG* unit. All non-degenerative configurations of black and white WS cells for such unit are presented in Fig.4a for square tessellation and in Fig.4b for hexagonal tessellation. In Fig.5a,b the process of scale renormalization is depicted for the specific distribution of *WS* cells. Mathematically, such a *RG* process can be described by a system of nonlinear equations (Eq.1). In the Table1, equations for probability r_n^k and their degeneracy numbers for classes of renormalization groups (Fig.4a,b) are presented. These equations comprise Eq.1a describing the *RG* process for an extra-cellular region. Eqs.(1c,d) were derived according to the rules given in the last column of Table1 and probability density (Eq.1b, where $\delta(x)$ is a Dirac delta-function).

3. Results: We input the microscopic parameters, X, taken from Table2 into the BS model to estimate lower (*L* superscript in notation, black square or hexagon in Fig.3a,b) and upper (*U* superscript in notation, white square or hexagon in Fig.3a,b) bounds of transverse diffusivity (*t* subscript in notation). The packing density of axons was taken into account. Then we were solving Eq.1 for different values of the extra-cellular volume fraction p. During the *RG* process, effective diffusion approaches the stable point $D_t^{U,n\to\infty} = D_t^{L,n\to\infty} = D_t^{n\to\infty}$ which depends on p and tissue tessellation type (Fig.6, red and black represent square and hexagonal packing). The first iteration step gives the classical results from the BS model. It is clear that as in classical model, as in enhanced model the packing density of axons influences the effective transversal diffusivity. In Fig.7 the sensitivity, S (Eq.3), of ADC_{eff} (Eq.2) to the various X microparameters changes in the biologically relevant limit $p \sim 0.2$ are presented. For comparison, we give *the classical BS* results. We denote X_1 as extracellular volume fraction, X_2 extracellular diffusion, X_3 myelin sheath diffusion, X_4 axon diffusion, X_5 mean axon size, X_6 mean myelin sheath size, X_7 extracellular proton density, X_8 myelin sheath proton density, X_9 axon proton density.

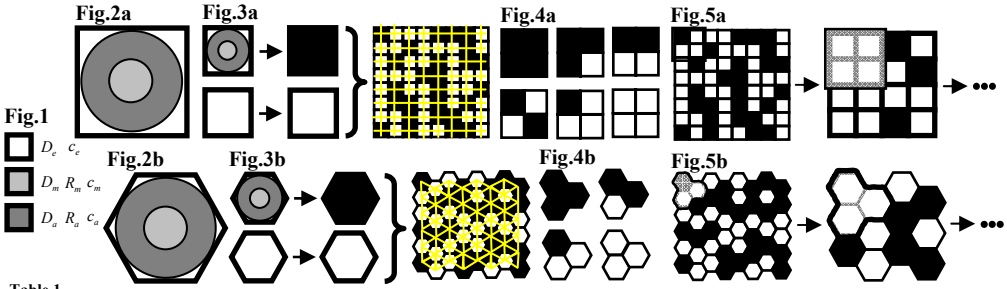

$$\begin{cases} p_{n+1} = \sum_k g_k r_n^k & (1a) \\ P_{n+1} = (1-p_n)\delta(D_t - D_t^{L,n}) + p_n \delta(D_t - D_t^{U,n}) & (1b) \\ D_t^{U,n+1} = \langle D_t^{U,n} \rangle & (1c) \\ D_t^{L,n+1} = \langle D_t^{L,n} \rangle & (1d) \end{cases}$$

$$ADC_{eff} = (2D_t^{n\to\infty} + D_l)/3 \quad (2)$$

$$S = \left|\partial \log(ADC_{eff}) / \partial \log(X)\right| \quad (3)$$

Table 1

Class	Probability, r_n^k	Degeneracy, g_k	Effective diffusivity, $D_t^{U/L,n+1}$
I □	$(1-p_n)^4$	1	$D_t^{L,n}$
II	$p_n^1(1-p_n)^3$	4	$\left(2D_t^{L,n}D_t^{U,n} + D_t^{L,n}(D_t^{L,n}+D_t^{U,n})\right)/2(D_t^{L,n}+D_t^{U,n})$
III	$p_n^2(1-p_n)^4$	4	$(2D_t^{L,n}D_t^{U,n})/(D_t^{L,n}+D_t^{U,n})$
IV	$p_n^2(1-p_n)^4$	2	$(D_t^{L,n}+D_t^{U,n})/2$
V	$p_n^3(1-p_n)^4$	4	$\left(2D_t^{L,n}D_t^{U,n} + D_t^{U,n}(D_t^{L,n}+D_t^{U,n})\right)/2(D_t^{L,n}+D_t^{U,n})$
VI	p_n^4	1	$D_t^{U,n}$
I ⬡	$(1-p_n)^3$	1	$D_t^{L,n}$
II	$p_n^1(1-p_n)^2$	3	$(2D_t^{L,n}D_t^{U,n})/(D_t^{L,n}+D_t^{U,n})$
III	$p_n^2(1-p_n)^1$	3	$(2D_t^{L,n}D_t^{U,n})/(D_t^{L,n}+D_t^{U,n})$
IV	p_n^3	1	$D_t^{U,n}$

Table 2

Parameter X	*Input value*	$X_5 = R_a$	$6.57*10^{-6}\,m.$
$X_1 = p$	[0;1]	$X_6 = R_m$	$4*10^{-6}\,m$
$X_2 = D_e$	$2*10^{-9}\,m^2/s$	$X_7 = c_e$	.95
$X_3 = D_m$	$.3*10^{-9}\,m^2/s$	$X_8 = c_m$	0.5
$X_4 = D_a$	$.75*10^{-9}\,m^2/s$	$X_9 = c_a$	0.88

Fig.6

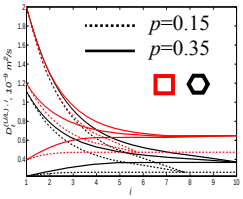

Fig.7

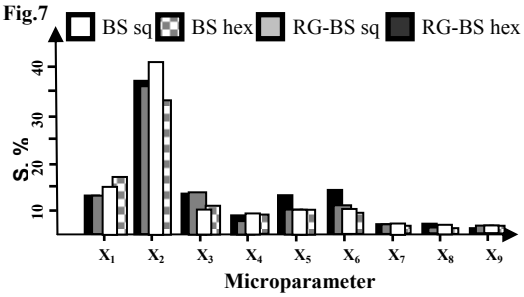

4. Discussion and conclusions: Using the *RG* method we have calculated the sensitivity of the ADC_{eff} to the different microparameters variations and packing densities of axons. We found that the ADC_{eff} exhibits it´s the strongest sensitivity to the extra-cellular volume fraction and diffusivity for all types of axon packing density. These findings suggest a possible mechanism to explain ADC_{eff} changes during neurodegenerative disease progression. The ADC_{eff} demonstrates more nonlinear behaviour vs changes in p due to blocking effects which are absent in an ordered model of the brain white matter.

5. References: [1] Sen P., Basser P., Biophys.J. 80(2005),2927.[2] Posnansky O., Shah N., J.Biol.Phys.34 (2008), 551. [3] Posnansky O., Shah N., ISMRM2009, 1360.